Influence of nuclear de-excitation on observables relevant for space exploration

Davide Mancusi [a,*], Alain Boudard [b], Joseph Cugnon [a], Jean-Christophe David [b], Sylvie Leray [b]

[a] *University of Liège, AGO Department, allée du 6 Août 17, bât. B5 B-4000 Liège 1, Belgium*

[b] *CEA/Saclay, Irfu/SPhN, 91191 Gif-sur-Yvette, Cedex, France*

Abstract

The composition of the space radiation environment inside spacecrafts is modified by the interaction with shielding material, with equipment and even with the astronauts' bodies. Accurate quantitative estimates of the effects of nuclear reactions are necessary, for example, for dose estimation and prediction of single-event-upset rates. To this end, it is necessary to construct predictive models for nuclear reactions, which usually consist of an intranuclear-cascade or quantum-molecular-dynamics stage, followed by a nuclear-de-excitation stage.

While it is generally acknowledged that it is necessary to accurately simulate the first reaction stage, transport-code users often neglect or underestimate the importance of the choice of the de-excitation code. The purpose of this work is to prove that the de-excitation model is in fact a non-negligible source of uncertainty for the prediction of several observables of crucial importance for space applications. For some particular observables, the systematic uncertainty due to the de-excitation model actually dominates the total uncertainty. Our point will be illustrated by making use of nucleon-nucleus calculations performed with several intranuclear-cascade/de-excitation models, such as the Liège Intranuclear Cascade model (INCL4) and Isabel (for the cascade part) and ABLA07, Dresner, GEM, GEMINI++ and SMM (on the de-excitation side).

Key words: nuclear de-excitation, intranuclear cascade, nuclear reactions, Monte-Carlo models
PACS: 87.10.Rt, 87.53.Bn, 24.10.Lx

* Corresponding author.
Email address: d.mancusi@ulg.ac.be (Davide Mancusi).

1 Introduction

Radiation exposure is generally recognised as one of the major hazards for the safety of spacecraft crews and equipment on long-term interplanetary missions. The most obvious countermeasure to date consists in shielding spacecraft and space stations with suitable materials, to reduce the dose absorbed by astronauts and thus the risk. However, the interaction of the space radiation environment with the shielding material generates an intense secondary radiation field, whose properties must be accurately assessed in order to make reliable risk predictions.

The secondary radiation field is typically due to proton-nucleus or nucleus-nucleus reactions at energies between a few hundred AMeV and several AGeV. Proton-nucleus reactions are especially frequent because of the high flux of Galactic Cosmic Ray (GCR) protons (87% of the total GCR baryonic flux) (Durante, 2002). Thus, the estimation of the quality of the secondary radiation field crucially depends on the availability of accurate nucleon-nucleus reaction models in the 0.1–10 GeV incident-energy range.

It is generally agreed that such reactions proceed in two stages: a fast ($\sim 10^{-22}$ s) dynamical stage generates an excited compound nucleus, which subsequently de-excites by emitting nucleons or light ions on a much longer time scale ($\sim 10^{-12}$ s). This distinction mirrors the different theoretical approaches that have been most successful in modelling the two stages. The fast stage of nucleon-induced reactions is traditionally described by intranuclear-cascade (INC) models (Serber, 1947), sometimes followed by an intermediate pre-equilibrium step; however, several other models (e.g. Quantum Molecolar Dynamics, Boltzmann-Uehling-Uhlenbeck, Vlasov-Uehling-Uhlenbeck) are often considered as well. The de-excitation of the compound-nucleus is usually handled by statistical decay or break-up models.

Transport-code users are generally aware of the great influence of the choice of the dynamical model on the calculation results. However, several observables are actually even more sensitive to the choice of the de-excitation model, which is generally just taken for granted. The goal of this work is to raise awareness about the importance of the choice of the de-excitation model for the estimation of several quantities relevant for radioprotection in space. We demonstrate that the systematic uncertainty due to the de-excitation stage can be as large as or larger than the uncertainty connected with the modelling of the dynamical stage.

To prove this point, we have performed thin-target nucleon-nucleus calculations with two INC models (INCL4, Isabel) coupled to five de-excitation codes (ABLA07, GEMINI++, GEM, SMM, Dresner). Thin-target calcu-

lations neglect transport of the reaction products in the surrounding material. Thick-target calculations would be better suited to assess the influence of de-excitation models. However, none of the major transport codes presently available offers a vast choice of nuclear-de-excitation models, which is indispensable for such a sensitivity study. On the other hand, the choice of nucleon-nucleus reactions is mainly motivated by the large cosmic-ray proton flux and by the abundance of hydrogen-rich materials in shielding. Moreover, the uncertainty connected with the dynamical stage is smaller for nucleon-nucleus than for nucleus-nucleus reactions, which can be affected by important collective phenomena such as bounce-off and squeeze-out. Thus, nucleon-nucleus reactions represent the best scenario to highlight the importance of de-excitation.

2 Model description

We will limit ourselves to give brief descriptions of the salient features of each model. The reader is referred to the relevant literature for further details.

2.1 Intranuclear-cascade models

The **Isabel** model (Yariv and Fraenkel, 1979, 1981) is a time-like intranuclear-cascade model that has widely contributed to the understanding of nucleon-nucleus and nucleus-nucleus collisions in the previous decades. It considers the target nucleus as a continuous medium (Fermi sea), which is perturbed by the collisions induced by the incoming cascading particles. ISABEL features one of the most detailed treatments of the $\Delta(1232)$ resonance.

The Liège Intranuclear-Cascade model (**INCL4**) (Boudard et al., 2002; Cugnon et al., 2010) is a modern addition to the INC family. Its main feature is that it represents the target nucleus as a collection of quasi-particles moving along straight trajectories in a potential well. It contains refined physics inspired by the optical-model phenomenology (e.g. energy- and isospin-dependent potentials for nucleons and pions), as well as a dynamical coalescence mechanism that makes the model applicable to the study of the observed emission of fast composite particles like deuterons, tritons and heavier nuclei. The $\Delta(1232)$ resonance is also treated in detail.

Both models can be applied to roughly the same incident-energy range (150 MeV–3 GeV).

ABLA07 (Ricciardi et al., 2009) is the latest version of the de-excitation code ABLA, originally developed by K.-H. Schmidt and his team (Gaimard and Schmidt, 1991). While the ABLA07 model is well known for its accurate treatment of fission, it has recently been extended to describe evaporation of intermediate-mass fragments (IMFs), multifragmentation and to include competition between particle and gamma-ray emission. An older version of the INCL4+ABLA cascade+de-excitation model is included in MCNPX and GEANT4.

The **Dresner** model (Dresner, 1962) is the default de-excitation option for the MCNPX transport code. It contains a simple Weisskopf-Ewing evaporation formalism, a simple Bohr-Wheeler fission model and utilises a Fermi break-up model to describe the de-excitation of light nuclei. It is nowadays unmaintained.

The Generalized Evaporation Model (**GEM**, Furihata, 2000) is a Japanese fission-evaporation code and the default option of the PHITS transport code (Iwase et al., 2002). Its uses the Weisskopf-Ewing evaporation formalism to describe the emission of nucleons and nuclei up to Mg.

The **GEMINI++** model, developed by R. Charity (Charity, 2008), is a binary de-excitation code, which is mostly notable for its fission-like description of IMF emission. Since it was originally developed to describe nucleus-nucleus reactions, GEMINI++ features an accurate treatment of orbital and intrinsic angular momentum. It is actually the only de-excitation model employed in this work that uses the Hauser-Feshbach evaporation formalism.

Finally, the Statistical Multifragmentation Model (**SMM**, Bondorf et al., 1995) is an actively developed code which combines the compound-nucleus de-excitation processes at low energy and simultaneous break-up at high energy. It has largely been used to study the behaviour and properties of nuclear matter at subnuclear density and it has been applied to multifragmentation reactions in astrophysics.

3 Results

We will now separately consider the influence of the choice of the de-excitation model on several observables of interest for radioprotection in space.

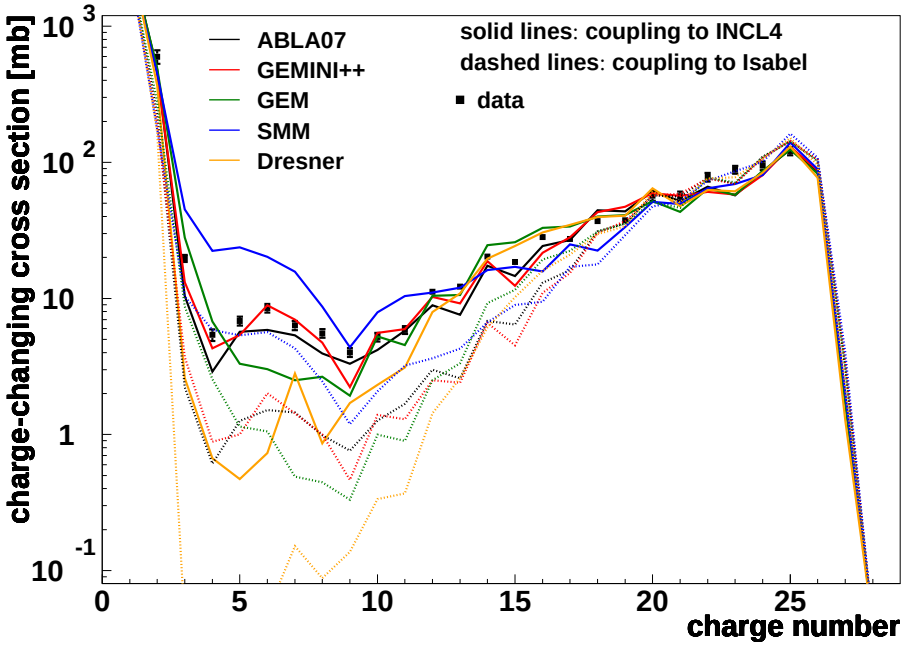

Fig. 1. Charge-changing cross sections for 1-GeV p+^{56}Fe. Cascade and de-excitation models are indicated by the dashing and the colouring, respectively. Experimental data from Napolitani et al. (2004); Villagrasa-Canton et al. (2007); Le Gentil et al. (2008).

3.1 Charge-changing cross sections

Since shielding materials are often rich in hydrogen, GCR nuclei frequently undergo nuclear reactions with target protons. Such reactions can easily be modelled in inverse kinematics (i.e. as proton-induced reactions) in the framework of cascade+de-excitation models. The charge-changing cross section for the GCR projectile is thus given by the corresponding cross section for the target nucleus in inverse kinematics.

Fig. 1 shows a comparison of charge-changing cross sections for 1-GeV p+^{56}Fe. The reaction has been selected because cosmic iron nuclei are responsible for a large fraction of the GCR equivalent dose; their charge-changing cross section thus need to be accurately predicted. The dashing style of the lines identifies the cascade model. The uncertainty connected with the choice of the de-excitation model can thus be estimated by comparing lines with the same dashing style. We observe that the spread is largest for the lightest fragments (IMFs). In the $3 \lesssim Z \lesssim 15$ charge range, the uncertainties connected with cascade and de-excitation are comparable. This can be explained by observing that this region is populated by cascade events with high excitation energies (several hundred MeV), which thus amplify the sensitivity to the details of the de-excitation model. At the same time, since events with high excitation energies are quite rare, their cross sections and distributions

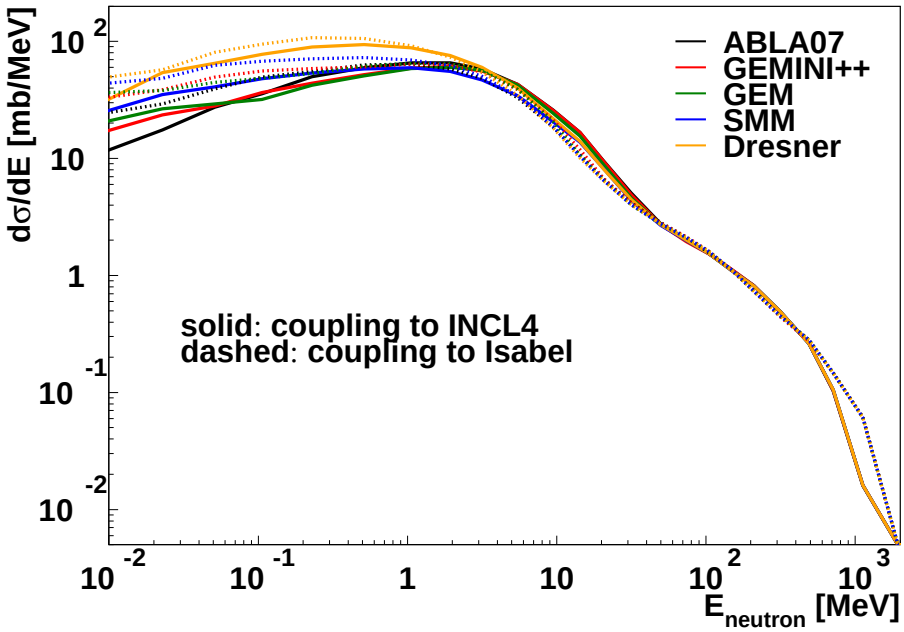

Fig. 2. Energy-differential neutron-production cross sections, for the 1-GeV p+^{27}Al reaction. Cascade and de-excitation models are indicated by the dashing and the colouring, respectively.

(and, thus, the $3 \lesssim Z \lesssim 15$ cross sections) are also sensitive to the choice of the cascade model.

3.2 Dose from secondary neutrons

We proceed by illustrating the influence of de-excitation models on secondary neutron production. Fig. 2 shows the calculated energy-differential neutron-production cross section for the 1-GeV p+^{27}Al reaction, which is taken as a representative of the reactions responsible for the creation of the strong secondary-neutron background in space vessels. It appears that de-excitation models mostly affect the low end of the spectrum, up to about 10–20 MeV. Above this energy, the cross section is entirely determined by the cascade stage.

Fig. 2 by itself is not conclusive about the importance of de-excitation models for the estimation of secondary-neutron doses. An accurate assessment would require a full three-dimensional transport calculation in a realistic geometry and with a realistic source. This is beyond the scope of this paper. We can nevertheless make a rough evaluation by using energy-dependent dose-conversion coefficients, such as those calculated by Sato et al. (2009) using the PHITS code and the ICRP/ICRU reference phantoms. Hence, we suppose that the ICRP/ICRU reference male phantom is irradiated isotropically by the neutrons fields depicted in Fig. 2. By multiplying the energy-differential

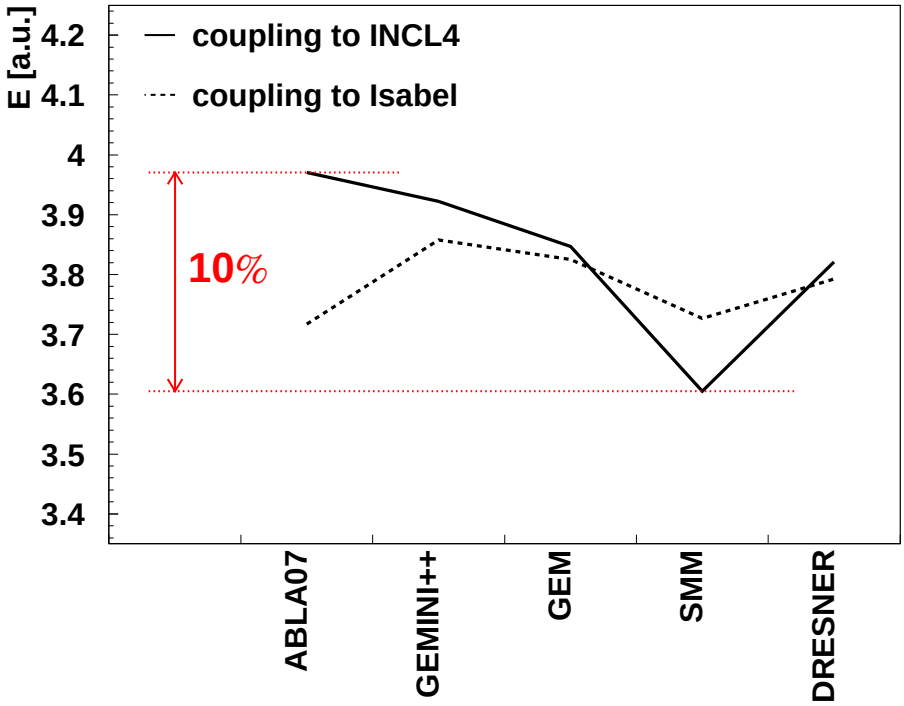

Fig. 3. Effective dose delivered by secondary neutrons of the 1-GeV p+^{27}Al reaction to the ICRP/ICRU male reference phantom, estimated using Sato et al.'s (2009) fluence-to-dose conversion coefficients for the isotropic irradiation geometry.

cross section by Sato et al.'s conversion coefficients and integrating over the neutron energy, we can obtain an estimate of the effective dose to the human body.

Fig. 3 shows the result of this procedure. Since the fluence-to-dose coefficients are small at low energy, the uncertainty connected with de-excitation is suppressed, but it is still of the same order of magnitude as the uncertainty due to cascade. Neither of them anyway exceeds 10%.

3.3 Dose from secondary protons

The results are radically different for secondary protons. It has been shown (Mancusi et al., 2007) that secondary protons can be responsible for a large increase in dose deposition (as much as 60%) after thick shields. This phenomenon is due to the large low-energy, high-LET fluxes of secondary protons produced in high-energy collisions.

We have again chosen 1-GeV p+^{27}Al as a representative reaction between space radiation and shielding material. The energy-differential cross sections for proton production are shown in Fig. 4. As in the case of neutrons, de-excitation yields dominate in the low-energy end of the spectrum. The uncer-

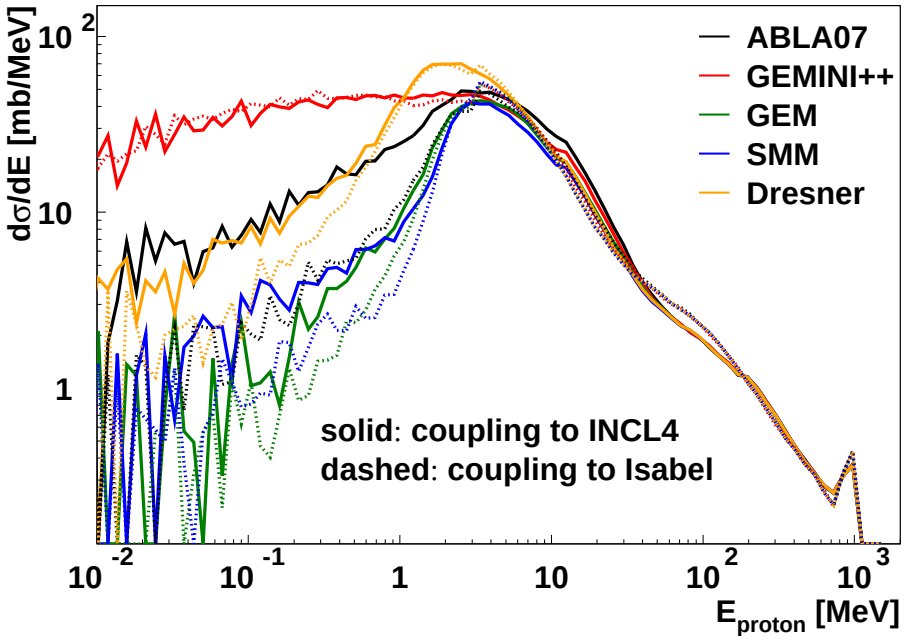

Fig. 4. Energy-differential proton-production cross sections, for the 1-GeV p+^{27}Al reaction. Cascade and de-excitation models are indicated by the dashing and the colouring, respectively.

tainty however appears to be much larger than for neutrons.

A rough estimate of the dose delivered by the depicted proton spectra can be obtained by assuming that protons deliver dose proportionally to their LET. This is approximately true for thin biological targets (e.g. skin) placed close to the shield. The approximation is less accurate for thick biological targets, where slowing-down and secondary reactions play an important role. In such a case, one could use fluence-to-dose conversion coefficients, as it was done in the previous section for neutrons.

If however the biological target is assumed to be thin, one can multiply the spectra in Fig. 4 by the ICRU reference LET-energy curves (International Commission on Radiation Units and Measurements, 1993) and integrate over the proton energy to obtain an estimate of the delivered dose. Since LET is a decreasing function of energy above ~ 0.1 MeV, the variance among the proton spectra will be amplified, contrarily to secondary neutron doses. Fig. 5 reveals that this result is found to be almost independent of the cascade model; on the other hand, different de-excitation models can yield doses that can differ by as much as 75%.

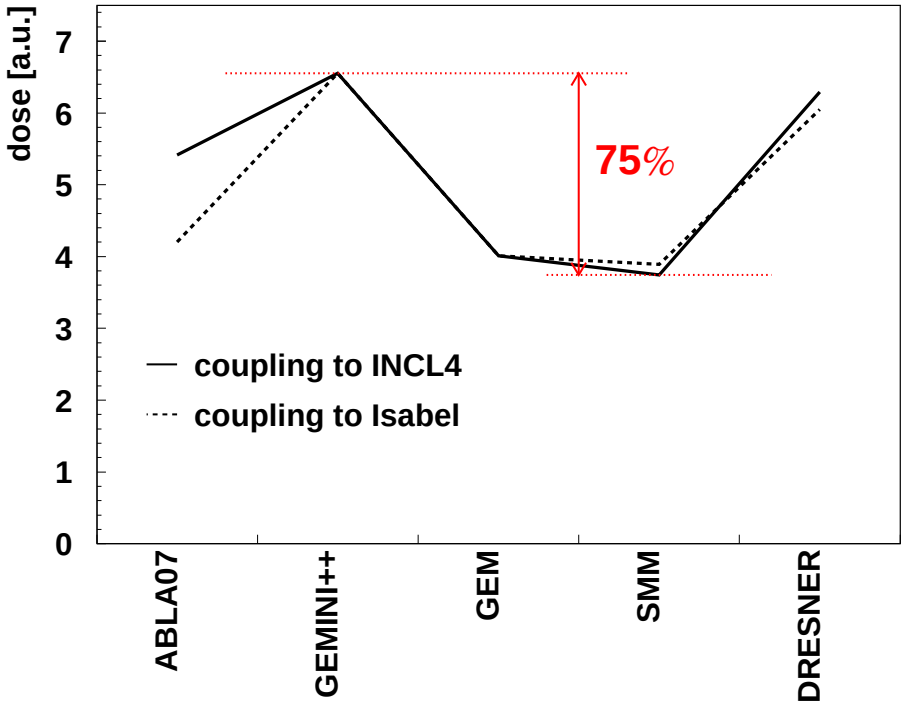

Fig. 5. Dose delivered to a thin biological target by secondary protons of the 1-GeV p+^{27}Al reaction.

3.4 Recoil-energy distributions

We finally turn to recoil-velocity distributions, which are important for the prediction of Single-Event-Upset (SEU) rates of electronic devices. SEUs are typically induced by nuclear reactions between secondary neutrons and silicon nuclei. Part of the recoil kinetic energy acquired by the target fragment is lost to the ionisation of the silicon wafer, which may upset the charge state of the electronic circuits therein contained. It is therefore crucial to be able to predict the recoil-energy distribution of the target fragments.

We have chosen 200-MeV n+^{28}Si as a representative reaction for the induction of SEUs. Fig. 6 shows differential cross sections as functions of the recoil kinetic energy for different charges of the recoiling fragments. Since the probability to induce a SEU increases with increasing LET of the particle, we focus here on the nuclei with the highest charges (top panel: $Z = 11$, 12; bottom panel: $Z \geq 13$). It is apparent that the main source of uncertainty here is the cascade model. Curves of the same dashing style tend to cluster together, while different de-excitation are only responsible for minor modulations. We thus conclude that recoil-velocity distributions for fragments close to the target are rather insensitive to the choice of the de-excitation model.

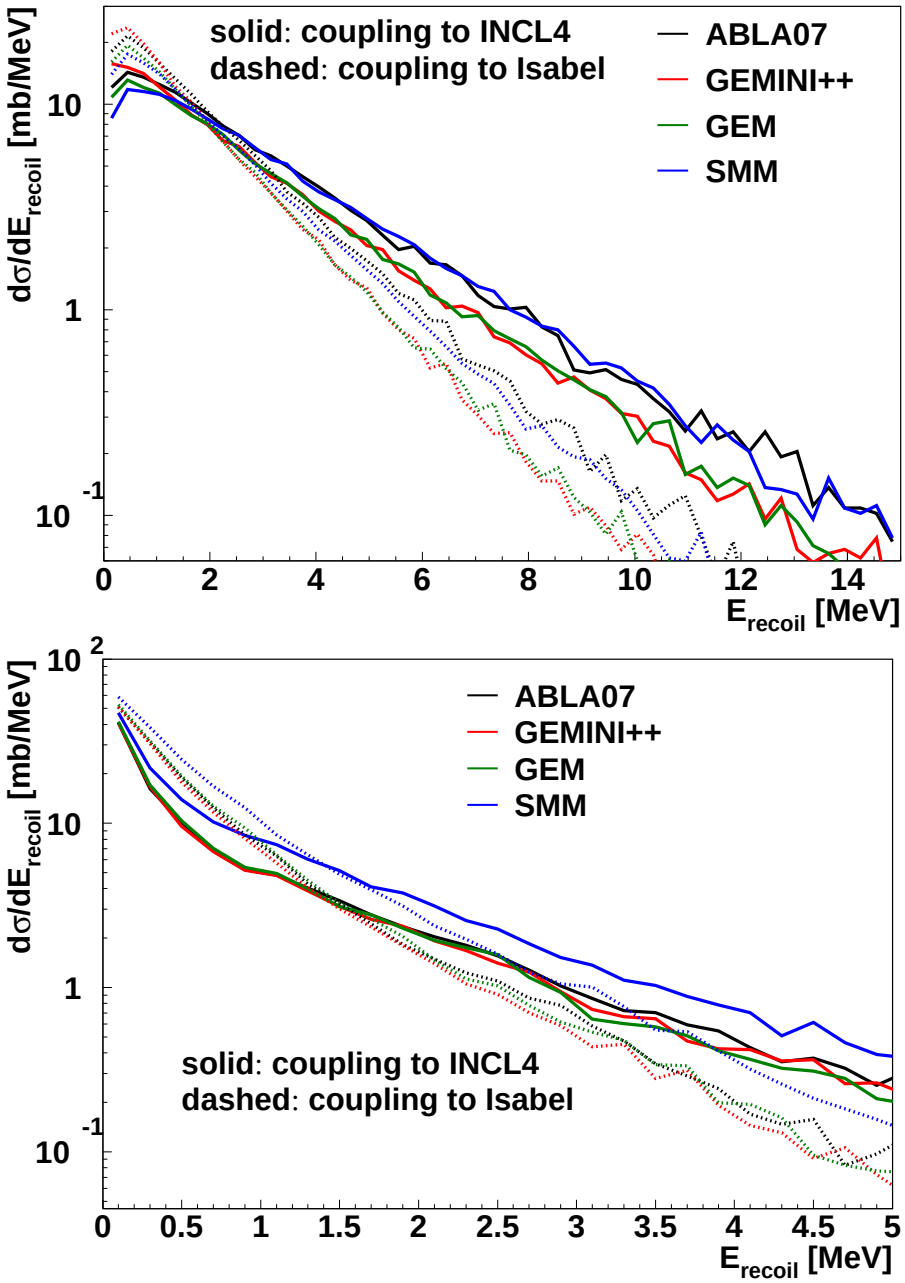

Fig. 6. Recoil-energy distributions induced by the 200-MeV n+^{28}Si reactions. Top panel: fragments with charge number $Z = 11$, 12. Bottom panel: $Z \geq 13$. Cascade and de-excitation models are indicated by the dashing and the colouring, respectively.

4 Conclusions and perspectives

We have studied the influence of nuclear-de-excitation models on several observables of interest for radioprotection of humans and equipment in space. The analysis was performed in the framework of nucleon-nucleus reactions, using two different intranuclear-cascade models (INCL4, Isabel) to simu-

late the dynamical stage of the reaction. Five different de-excitation models (ABLA07, GEMINI++, GEM, SMM, Dresner) were selected.

We have proved that the choice of the de-excitation model introduces a non-negligible uncertainty on charge-changing cross sections for intermediate-mass fragments. Likewise, secondary-proton doses in thin biological targets can vary by as much as 75% with the choice of the de-excitation model. On the other hand, recoil-velocity distributions, which are essential for the determination of single-event-upset rates, and secondary-neutron doses are less sensitive to the de-excitation stage. One can summarise these results by observing that the observables that are sensitive to de-excitation are typical of violent nuclear reactions. Very central collisions indeed lead to high excitation energies at the end of the cascade stage, which amplify the sensitivity to the parameters and assumptions of the de-excitation models.

The influence of de-excitation models should be further investigated by performing thick-target calculations with realistic geometries and radiation sources. However, this requires several de-excitation models to be available within the same transport code. None of the major transport codes offer this possibility today. Hence, we encourage transport-code developers to consider the inclusion of several de-excitation models.

Finally, it is less clear whether our conclusions would still hold in the context of nucleus-nucleus reactions, whose importance in space is capital because of the large dose fraction delivered by GCR heavy ions. The strategy outlined in the present paper can be applied to nucleus-nucleus reactions as well, provided that several dynamical reaction models are available.

References

Bondorf, J. P., Botvina, A. S., Iljinov, A. S., Mishustin, I. N., Sneppen, K., June 1995. Statistical multifragmentation of nuclei. Phys. Rep. 257 (3), 133–221.

Boudard, A., Cugnon, J., Leray, S., Volant, C., October 2002. Intranuclear cascade model for a comprehensive description of spallation reaction data. Phys. Rev. C 66 (4), 044615.

Charity, R. J., 2008. GEMINI: a code to simulate the decay of a compound nucleus by a series of binary decays. In: Joint ICTP-IAEA Advanced Workshop on Model Codes for Spallation Reactions. IAEA, Trieste, Italy, p. 139, report INDC(NDC)-0530.

Cugnon, J., Boudard, A., Leray, S., Mancusi, D., 26-30 April 2010. New features of the INCL4 model for spallation reactions. In: International Conference on Nuclear Data for Science and Technology. Korean Nuclear Society and Korean Atomic Energy Research Institute, Jeju Island, Korea.

Dresner, L., April 1962. EVAP: a FORTRAN program for calculating the evaporation of various particles from excited compound nuclei. ORNL report ORNL-TM-196, Oak Ridge National Laboratory, Oak Ridge, TN, U.S.A.

Durante, M., August 2002. Radiation protection in space. Riv. Nuovo Cimento 25 (8), 1–70.

Furihata, S., November 2000. Statistical analysis of light fragment production from medium energy proton-induced reactions. Nucl. Instr. Meth. B 171 (3), 251–258.

Gaimard, J.-J., Schmidt, K.-H., September 1991. A reexamination of the abrasion-ablation model for the description of the nuclear fragmentation reaction. Nucl. Phys. A 531 (3–4), 709–745.

International Commission on Radiation Units and Measurements (Ed.), 1993. Stopping Powers and Ranges of Protons and Alpha Particles. Journal of the ICRU. Oxford Journals, ICRU report 49.

Iwase, H., Niita, K., Nakamura, T., 2002. Development of general-purpose particle and heavy ion transport Monte Carlo code. J. Nucl. Sci. Technol. 39 (11), 1142–1151.

Le Gentil, E., et al., January 2008. Coincidence measurement of residues and light particles in the reaction ^{56}Fe+p at 1 GeV per nucleon with the spallation reactions setup SPALADIN. Phys. Rev. Lett. 100 (2), 022701.

Mancusi, D., Bertucci, A., Gialanella, G., Grossi, G., Manti, L., Pugliese, M., Rusek, A., Scampoli, P., Sihver, L., Durante, M., 2007. Comparison of aluminum and lucite for shielding against 1 GeV protons. Adv. Space Res. 40 (4), 581–585.

Napolitani, P., Schmidt, K.-H., Botvina, A. S., Rejmund, F., Tassan-Got, L., Villagrasa, C., November 2004. High-resolution velocity measurements on fully identified light nuclides produced in ^{56}Fe+hydrogen and ^{56}Fe+titanium systems. Phys. Rev. C 70 (5), 054607.

Ricciardi, M. V., Kelić, A., Schmidt, K.-H., May 2009. Results obtained with ABLA07. In: Proceedings to the Satellite Meeting on Nuclear Spallation Reactions, International Topical Meeting on Nuclear Research Applications and Utilization of Accelerators. IAEA, Vienna, Austria.

Sato, T., Endo, A., Zankl, M., Petoussi-Henss, N., Niita, K., April 2009. Fluence-to-dose conversion coefficients for neutrons and protons calculated using the PHITS code and ICRP/ICRU adult reference computational phantoms. Phys. Med. Biol. 54 (7), 1997–2014.

Serber, R., December 1947. Nuclear reactions at high energies. Phys. Rev. 72 (11), 1114–1115.

Villagrasa-Canton, C., et al., April 2007. Spallation residues in the reaction ^{56}Fe+p at 0.3A, 0.5A, 0.75A, 1.0A, and 1.5A GeV. Phys. Rev. C 75 (4), 044603.

Yariv, Y., Fraenkel, Z., December 1979. Intranuclear cascade calculation of high-energy heavy-ion interactions. Phys. Rev. C 20 (6), 2227–2243.

Yariv, Y., Fraenkel, Z., August 1981. Intranuclear cascade calculation of high energy heavy ion collisions: Effect of interactions between cascade particles.

Phys. Rev. C 24 (2), 488–494.